



OPEN ACCESS

ORIGINAL ARTICLE

Targeting the gut microbiota with inulin-type fructans: preclinical demonstration of a novel approach in the management of endothelial dysfunction

Emilie Catry,¹ Laure B Bindels,¹ Anne Tailleux,^{2,3,4,5} Sophie Lestavel,^{2,3,4,5} Audrey M Neyrinck,¹ Jean-François Goossens,^{6,7} Irina Lobysheva,⁸ Hubert Plovier,^{1,9} Ahmed Essaghir,¹⁰ Jean-Baptiste Demoulin,¹⁰ Caroline Bouzin,¹¹ Barbara D Pachikian,¹ Patrice D Cani,^{1,9} Bart Staels,^{2,3,4,5} Chantal Dessy,⁸ Nathalie M Delzenne¹

► Additional material is published online only. To view please visit the journal online (<http://dx.doi.org/10.1136/gutjnl-2016-313316>).

For numbered affiliations see end of article.

Correspondence to

Professor Nathalie M Delzenne, Metabolism and Nutrition Research Group, Louvain Drug Research Institute, Université catholique de Louvain, 73, avenue E. Mounier, B01.73.11, Brussels 1200, Belgium; nathalie.delzenne@uclouvain.be

CD and NMD contributed equally.

Received 27 October 2016
Revised 17 February 2017
Accepted 20 February 2017
Published Online First
04 April 2017



► <http://dx.doi.org/10.1136/gutjnl-2017-314012>



CrossMark

To cite: Catry E, Bindels LB, Tailleux A, et al. *Gut* 2018;**67**:271–283.

ABSTRACT

Objective To investigate the beneficial role of prebiotics on endothelial dysfunction, an early key marker of cardiovascular diseases, in an original mouse model linking steatosis and endothelial dysfunction.

Design We examined the contribution of the gut microbiota to vascular dysfunction observed in apolipoprotein E knockout (ApoE^{−/−}) mice fed an n-3 polyunsaturated fatty acid (PUFA)-depleted diet for 12 weeks with or without inulin-type fructans (ITFs) supplementation for the last 15 days. Mesenteric and carotid arteries were isolated to evaluate endothelium-dependent relaxation ex vivo. Caecal microbiota composition (Illumina Sequencing of the 16S rRNA gene) and key pathways/mediators involved in the control of vascular function, including bile acid (BA) profiling, gut and liver key gene expression, nitric oxide and gut hormones production were also assessed.

Results ITF supplementation totally reverses endothelial dysfunction in mesenteric and carotid arteries of n-3 PUFA-depleted ApoE^{−/−} mice via activation of the nitric oxide (NO) synthase/NO pathway. Gut microbiota changes induced by prebiotic treatment consist in increased NO-producing bacteria, replenishment of abundance in *Akkermansia* and decreased abundance in bacterial taxa involved in secondary BA synthesis. Changes in gut and liver gene expression also occur upon ITFs suggesting increased glucagon-like peptide 1 production and BA turnover as drivers of endothelium function preservation.

Conclusions We demonstrate for the first time that ITF improve endothelial dysfunction, implicating a short-term adaptation of both gut microbiota and key gut peptides. If confirmed in humans, prebiotics could be proposed as a novel approach in the prevention of metabolic disorders-related cardiovascular diseases.

INTRODUCTION

Nutritional quality of diets underlies or exacerbates several chronic pathologies, including cardiovascular disease (CVD).^{1 2} Western diets that are mainly characterised by an imbalance between energy and fat intakes and a lack of key nutrients,

Significance of this study

What is already known on this subject?

- Metabolic diseases such as diabetes or non-alcoholic fatty liver disease are associated with macro- and microcirculation and microcirculation damages, initiating an impairment of endothelium-dependent relaxation, a primary driver of cardiovascular diseases.
- Dietary n-3 polyunsaturated fatty acid (PUFA) depletion induces hepatic steatosis and accelerates the development of endothelial dysfunction in mesenteric arteries of apolipoprotein E knockout (ApoE^{−/−}) mice.
- Gut microbiota plays a crucial role in the control of host intestinal functions, through the release and/or transformation of metabolites (eg, bile acids and short chain fatty acids) which regulate gut endocrine function, these pathways being mostly studied in the context of obesity.

What are the new findings?

- Inulin-type fructans (ITFs) are able to restore the endothelial dysfunction observed in mesenteric and carotid arteries from n-3 PUFA-depleted ApoE^{−/−} mice without impacting adiposity.
- The improvement of vascular dysfunction by ITF is linked to an activation of the NOS/NO pathway pathway, which could be dependent on events occurring at the microbiota level (increase in NO-producing bacteria) and/or host level (changes in bile acid composition, increase in the L cells density and in glucagon-like peptide 1 production, both acting on the NOS/NO pathway).
- Our data support, for the first time in the context of vascular dysfunction, the concept that changing the gut microbiota has a profound influence on key intestinal functions involved in host cardiometabolic health.

Significance of this study

How might it impact on clinical practice in the foreseeable future?

- Intrahepatic and mesenteric endothelial dysfunctions in metabolic diseases are known as actor and predictor of deleterious cardiovascular consequences. If the positive impact of ITF on endothelial dysfunction is confirmed in human studies, they could be proposed as a novel approach in the prevention and the management of metabolic disorders-related cardiovascular diseases.

like fibres and n-3 polyunsaturated fatty acids (PUFAs), enhance CVD risk.³

An early key marker of CVD is endothelial dysfunction, reflecting the integrated effects of risk factors on the vasculature.⁴ It originates from the incapacity of endothelial cells to balance synthesis and release of deleterious versus protective mediators, among which nitric oxide (NO) is the most important. Endothelial dysfunction is characterised by reduced vasodilation in response to endothelial stimuli.⁵ Interestingly, besides inducing metabolic alterations, nutritional depletion in n-3 PUFAs for 12 weeks accelerates the process of endothelial dysfunction in apolipoprotein E knockout (*Apoe*^{-/-}) mice.⁶

The gut microbiota comprises the trillions of commensal micro-organisms residing within our intestines.⁷ All the genes of this community – the gut microbiome – represent at least 100-fold more genes than the host genome.⁸ The gut microbiota may be considered as an ‘external’ organ playing an important role in host physiology and metabolism. Only a few studies focus on the role of gut microbiota in the context of CVDs. Interestingly, Stepankova *et al*⁹ reported that germ-free *Apoe*^{-/-} mice developed more aortic atherosclerotic plaques compared with conventionally raised *Apoe*^{-/-} mice fed the same low standard cholesterol diet. Rault-Nania *et al*¹⁰ demonstrated that inulin treatment attenuated atherosclerosis in *Apoe*^{-/-} mice, however, the mechanism was unexplored. We found that inulin-type fructans (ITFs) feeding increases the abundance of *Akkermansia muciniphila* in obese mice,^{11 12} a bacterium known to reduce atherosclerotic lesions induced by a Western diet in mice.¹³

For years, we and others have proven that dietary fibre supplementation can modulate the composition of the gut microbiota, and thus interact with host physiology.^{14 15} This is particularly the case for ITFs, which are classified as prebiotics. Prebiotics are ‘non-digestible compounds that through metabolism by microorganisms in the gut, modulate the composition and/or activity of the gut microbiota, thereby conferring a beneficial physiological effect on host’.¹⁶ We have additionally shown that ITFs are able to lower hepatic steatosis in n-3 PUFA-depleted wild-type (WT) mice, by modulating gene expression in the liver.¹⁷

The microcirculation (e.g. the enteric arterial tree) plays key roles in the metabolic diseases progression.^{18 19} We have evaluated for the first time the influence of ITFs in a model in which endothelial dysfunction appears independently of obesity and inflammation,⁶ both being affected by ITFs. Our model allows to point out molecular mechanisms by which changes in gut microbiota might remedy the enteric vascular dysfunction.

MATERIALS AND METHODS

Additional protocols and complete procedures are described in the online supplementary material and methods section.

Animals

Nine-week-old male C57Bl/6J (WT) and *Apoe*^{-/-} (KO) mice (Charles River Laboratories, L'Arbresle, France) were fed an n-3 PUFA-depleted (DEF) diet (D08041806, Research Diets, New Brunswick, New Jersey, USA) for 12 weeks. At 10 weeks of n-3 PUFA depletion, for each genotype, mice were separated in two groups and supplemented or not with ITFs (OraftiP95, Tienen, Belgium) at 250 mg/mouse/day in the drinking water.

Measurement of vascular contraction and relaxation

Endothelium-dependent relaxation was evaluated by cumulative addition of acetylcholine (ACh) (from 10⁻⁸ M to 3.10⁻⁵ M) on precontracted arteries with a high KCl solution, in presence or absence of Nω-Nitro-L-arginine methyl ester (L-NAME) (100 μM).

Microarray analysis

Equal amounts of RNA from eight mice were pooled within each group. Microarrays were performed as previously described.²⁰ Data are available under GEO accession number GSE87603.

Gut microbiota analyses

Genomic DNA was extracted from caecal content using a QIAamp DNA Stool Mini Kit (Qiagen, Germany), including a bead-beating step. Illumina sequencing was performed as previously described.²¹ The V5-V6 region of the 16S rRNA gene was amplified by PCR with modified primers. The amplicons were purified, quantified and sequenced using an Illumina Miseq to produce 2×300-bp sequencing products at the University of Minnesota Genomics Center. Initial quality filtering of the reads was conducted with Illumina Software, yielding an average of 66766 pass-filter reads per sample. Quality scores were visualised, and reads were trimmed to 220 bp (R1) and 200 bp (R2). The reads were merged with the merge-Illumina-pairs application.²² For samples with >25 000 merged reads, a subset of 25 000 reads was randomly selected using Mothur 1.25.0²³ to avoid large disparities in the number of sequences. Subsequently, the UPARSE pipeline implemented in USEARCH V7.0.1001²⁴ was used to further process the sequences. Putative chimaeras were identified against the Gold reference database and removed. Clustering was performed with a 98% similarity cut-off to designate operational taxonomic units (OTUs). Non-chimerical sequences were also subjected to taxonomic classification using the RDP MultiClassifier 1.1 from the Ribosomal Database Project²⁵ for phylum to genus characterisation of the faecal microbiome. The phylotypes were computed as per cent proportions based on the total number of sequences in each sample.

Statistical analysis

Results are presented as mean±SEM. Statistical differences were assessed by one-way or two-way analysis of variance followed by Tukey's or Bonferroni's post-tests. Unpaired *t*-test was used for comparison between KO DEF and KO DEF ITF mice. Data with superscript symbol (* vs WT DEF, \$ vs WT DEF ITF or # vs KO DEF) were significantly different (*p*<0.05). Statistical analyses were performed using GraphPad Prism V5.00 for windows.

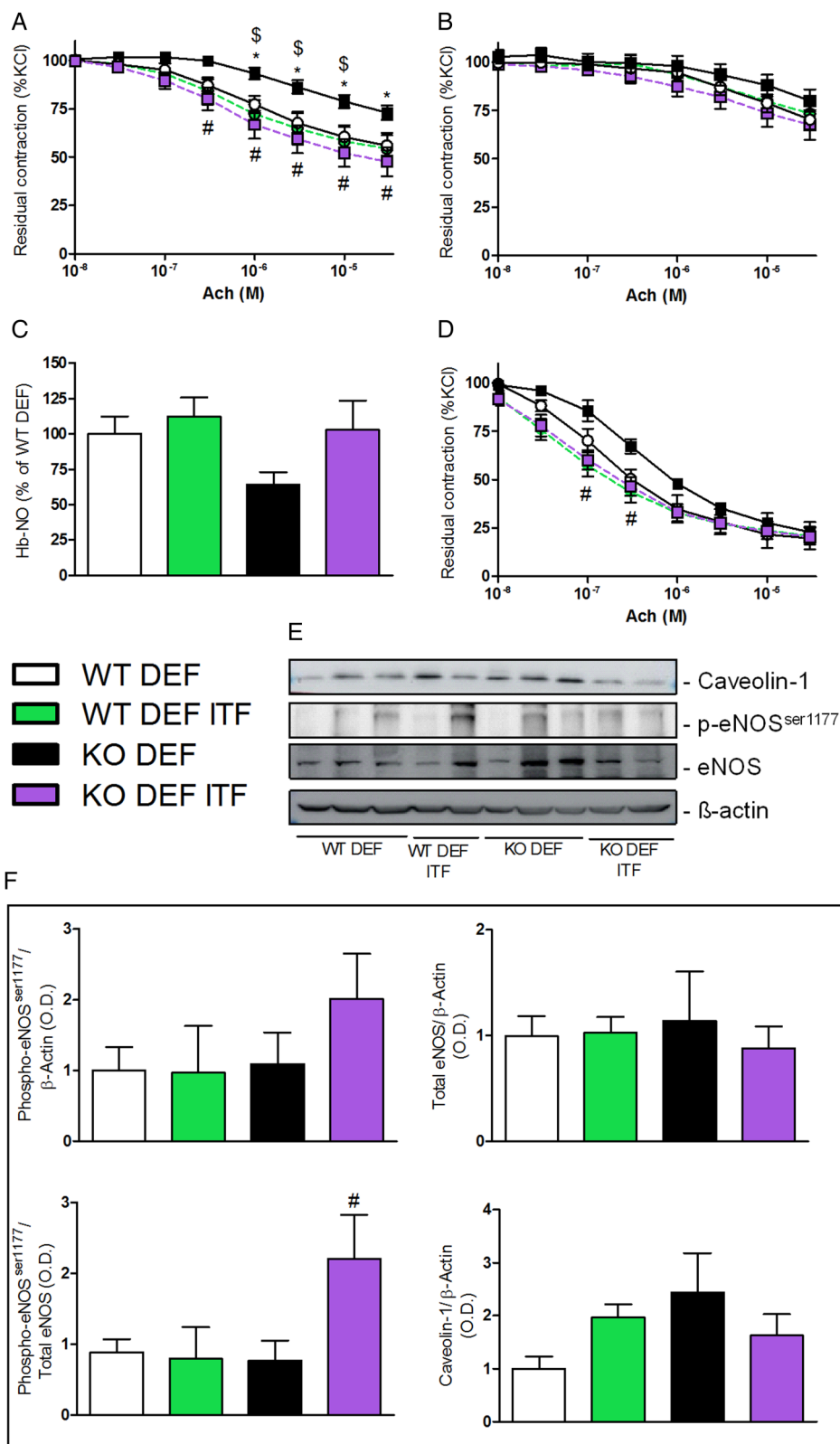
RESULTS

Endothelial dysfunction is improved by ITF treatment through the activation of the NO synthase/NO pathway

As expected, mesenteric arteries isolated from n-3 PUFA-depleted Apoe^{-/-} mice (KO DEF) developed a significant endothelial dysfunction, attested by the reduced vasodilation to cumulative doses of Ach (figure 1A). Fifteen days of ITF supplementation significantly improved the relaxation of mesenteric

arteries isolated from n-3 PUFA-depleted Apoe^{-/-} mice supplemented with ITFs (KO DEF ITF) as compared with WT mice, treated or not (figure 1A). The non-selective NO synthase (NOS) inhibitor (L-NAME) completely blunted the relaxation in mesenteric resistance arteries independently of diet or genetic background, suggesting an implication of the NOS/NO pathway (figure 1B). In line with endothelial dysfunction, KO DEF mice displayed a 40% decrease in haem-nitrosylated haemoglobin

Figure 1 Endothelium-dependent relaxation. (A) Endothelium-dependent relaxation of precontracted mesenteric arteries (N=7–11) and (B) in presence of nitric oxide synthase (NOS) inhibitor (N ω -Nitro-L-arginine methyl ester (L-NAME), 100 μ M) (N=7–11). (C) Circulating haem-nitrosylated haemoglobin (Hb-NO) levels (N=15–18). (D) Endothelium-dependent relaxation of precontracted carotid arteries (N=5–6). (E) Western blot analyses on mesenteric arteries with anti-caveolin-1, anti-phosphorylated endothelial NOS (eNOS)^{ser1177}, anti-eNOS and anti- β actin. (F) Densitometric analyses of stained membranes (N=5–6). Data are expressed as mean \pm SEM and analysed by one-way or two-way analysis of variance followed by Tukey's or Bonferroni's post-tests: * versus WT DEF, \$ versus WT DEF ITF, # versus KO DEF.



(Hb-NO) levels, measured by electron paramagnetic resonance, as compared with WT DEF mice. Interestingly, ITF treatment restored Hb-NO to similar levels as measured in WT mice (figure 1C). We investigated the relaxation profile of carotid arteries, another type of vessel, conductance versus resistance arteries, and at distance from the gut. The beneficial effects of ITFs on mesenteric arteries relaxation were also observed in carotid arteries isolated from KO DEF ITF mice (figure 1D). We used western blotting to assess total endothelial NOS (eNOS) as well as its activating serine 1177 phosphorylated form (p-eNOS^{ser1177}) along with its allosteric regulator, caveolin-1 (figure 1E). eNOS phosphorylation was twofold higher in mesenteric arteries from KO DEF ITF mice compared with KO DEF mice, while total eNOS protein was not significantly affected by genotype and/or diet. This resulted in a significantly increased p-eNOS^{ser1177}/eNOS ratio in mesenteric arteries isolated from KO DEF ITF mice, compared with samples from KO DEF ITF. In accordance with previous observations,²⁶ we observed a slight increase in caveolin-1 abundance in KO DEF versus WT DEF (figure 1F).

ITF treatment impacts resting parameters and vascular reactivity in mesenteric arteries

Resting tone was significantly higher in mesenteric arteries isolated from KO DEF ITF mice, compared with untreated mice (figure 2A). This effect was associated with a significantly larger mean arterial diameter, as compared with WT DEF mice (figure 2B). Mesenteric arteries from KO DEF ITF mice contracted significantly more in response to KCl-enriched solution (50 mM) compared with all other groups (figure 2C). Intima-media thickness in mesenteric arteries from KO DEF mice was significantly reduced in comparison with either treated or untreated WT DEF mice (figure 2D,E). Interestingly, media remodelling was completely reversed by 15 days of ITF supplementation.

Microarray analysis highlights several pathways affected by ITF treatment

To identify the mechanisms underlying the improvement in endothelial function by ITF treatment, we analysed we analysed caecal gene expression profiles by microarray (figure 3). Further comparison focused on KO genotypes in which most effects

Figure 2 Resting parameters and vascular reactivity of mesenteric arteries. (A) Resting tone (N=7–11). (B) Normalised vessel diameter (N=7–11). (C) Maximal contraction in response of KCl-enriched solution (50 mM) (N=7–11). (D) Intima-media thickness of first order mesenteric arteries (N=6–8) and (E) representative pictures (scale bar=100 μ m). Data are expressed as mean \pm SEM and analysed by one-way analysis of variance followed by Tukey's post-tests: * versus WT DEF, \$ versus WT DEF ITF, # versus KO DEF.

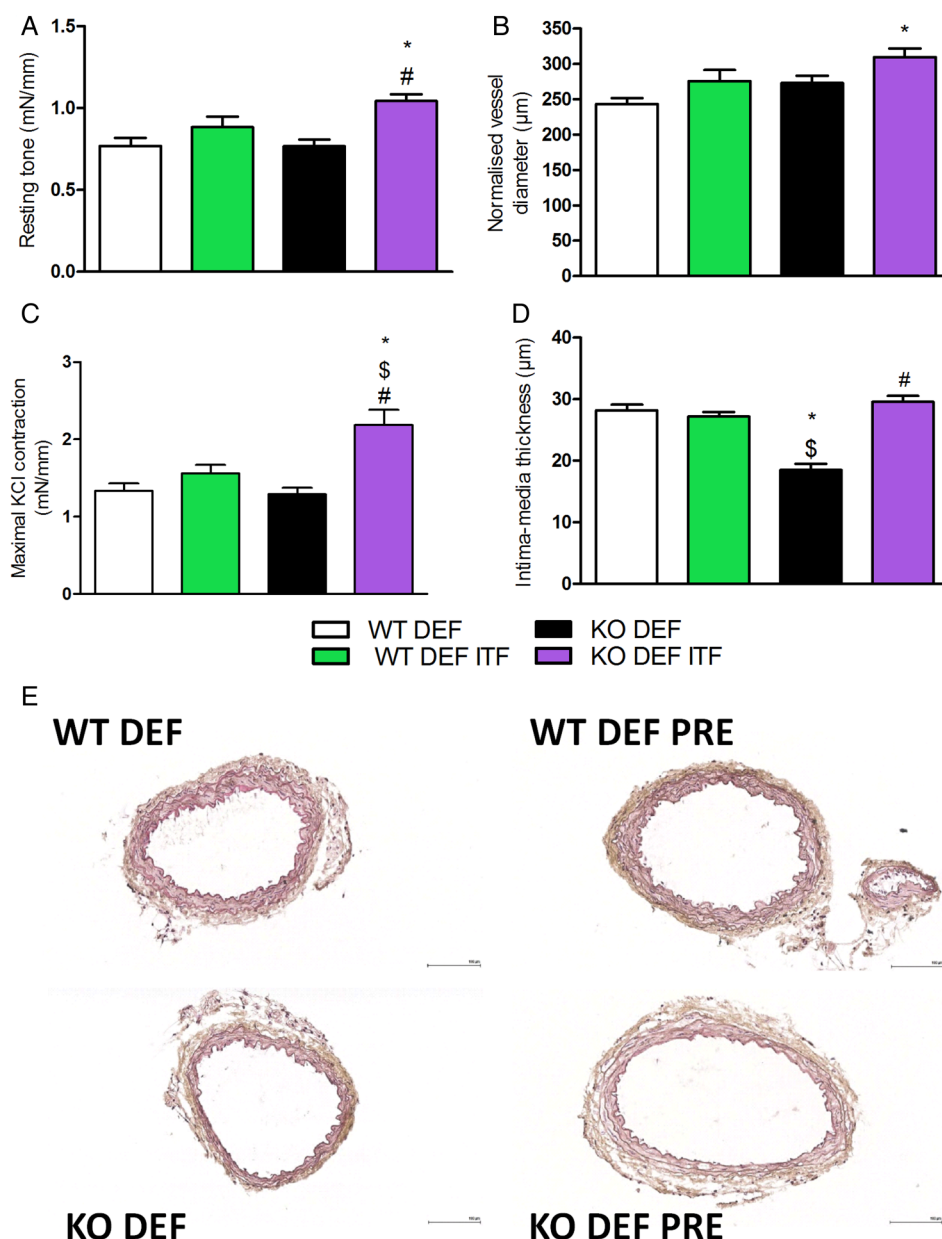
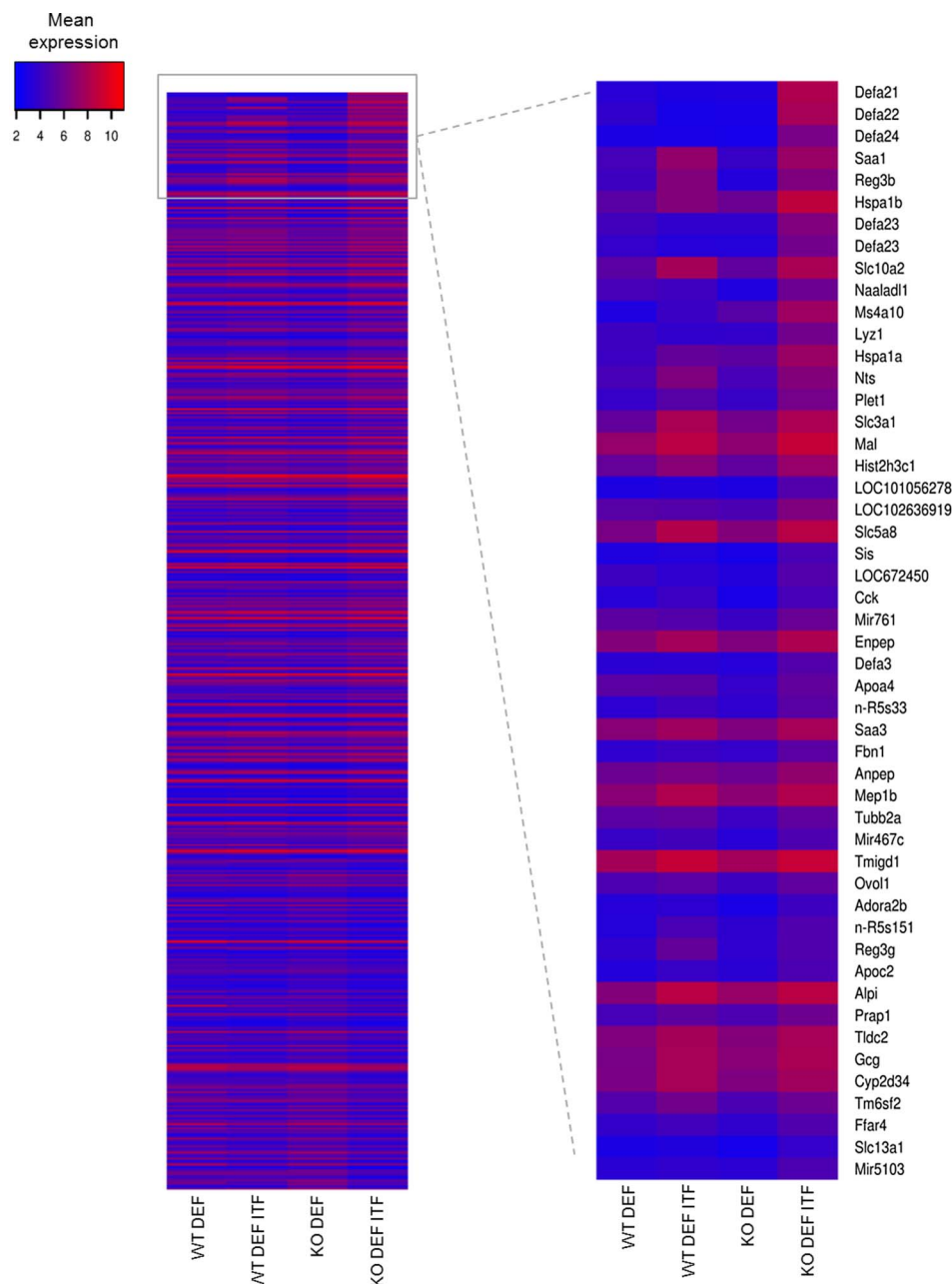


Figure 3 Microarray analysis on the caecal tissue. Heatmap from microarray analysis representing the top 50 upregulated genes in the caecum, based on the list of genes upregulated by 1.5-fold between KO DEF ITF and KO DEF mice. Data are expressed as mean \log_2 expression.



were observed. ITF treatment led to an increased expression in (1) various antimicrobial peptides (e.g. *Defa*, *Reg3 β* , *SAA1*, *SAA3*), (2) genes involved in bile acid (BA) metabolism (*Slc10a2*), (3) aminopeptidases (*Anpep*, *Enpep*) and (4) (pro)hormones, neurotensin (*Nts*) and proglucagon (*Gcg*). Quantitative PCR analyses confirmed these microarray data (see online supplementary figure S1).

ITF treatment profoundly modifies the gut microbiota composition in WT and KO mice

Shannon and Simpson Indexes (figure 4A), representing richness and evenness, were significantly decreased in KO DEF ITF mice compared with KO DEF mice just as well as Evenness Indexes (Simpson Evenness and Heip Indexes, figure 4B). However, the richness (measured using Chao1 and Observed Species Indexes, figure 4C) was not significantly modified in any groups. The β -diversity was also profoundly changed in ITF-treated WT and KO mice, as observed in the principal coordinates analysis

(PCoA) of the Morisita-Horn Index (figure 4D) and the weighted UniFrac Index (figure 4E) at the OTU level. The three first principal coordinates respectively explained 56% and 66% of the variation observed between all the groups. In the two PCoA, we observed clustering for ITF-treated versus untreated mice, independently of genotype. At the phyla level (figure 4F), several shifts clearly operated following ITF supplementation in the two genotypes such as a decreased abundance of the Firmicutes phylum and an increased abundance of the Bacteroidetes, Actinobacteria and Proteobacteria phyla. Intriguingly, KO DEF mice presented a lower relative abundance of the Verrucomicrobia phylum compared with WT DEF mice and ITFs were able to restore its abundance (figure 4F). Parametrical analysis at lower taxonomical levels revealed additional changes. ITF had growth-fostering effects on the Erysipelotrichaceae family and *Bifidobacterium* genus in both genotypes. In line with the observations at the phylum level, abundance of *Akkermansia* genus was drastically decreased

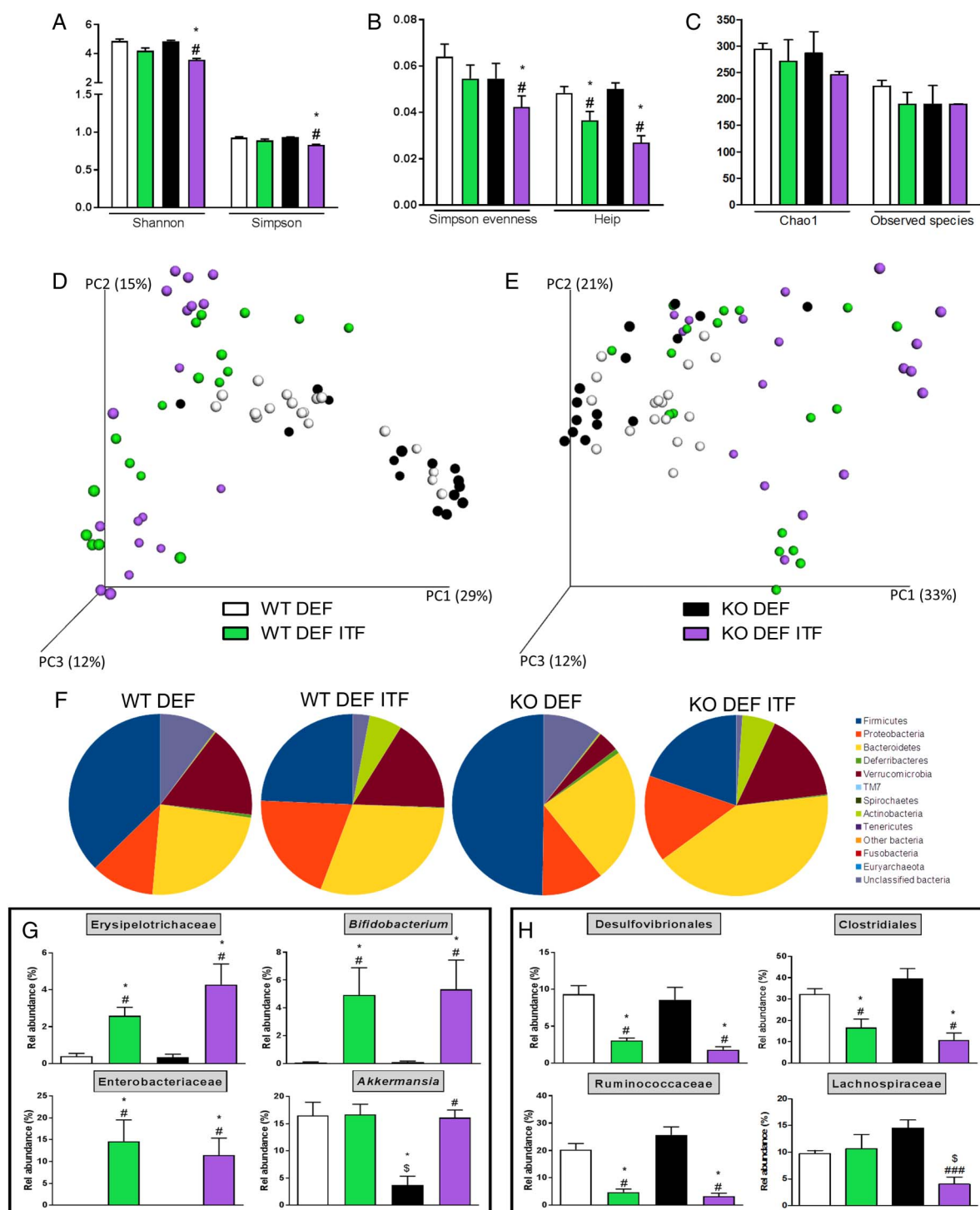
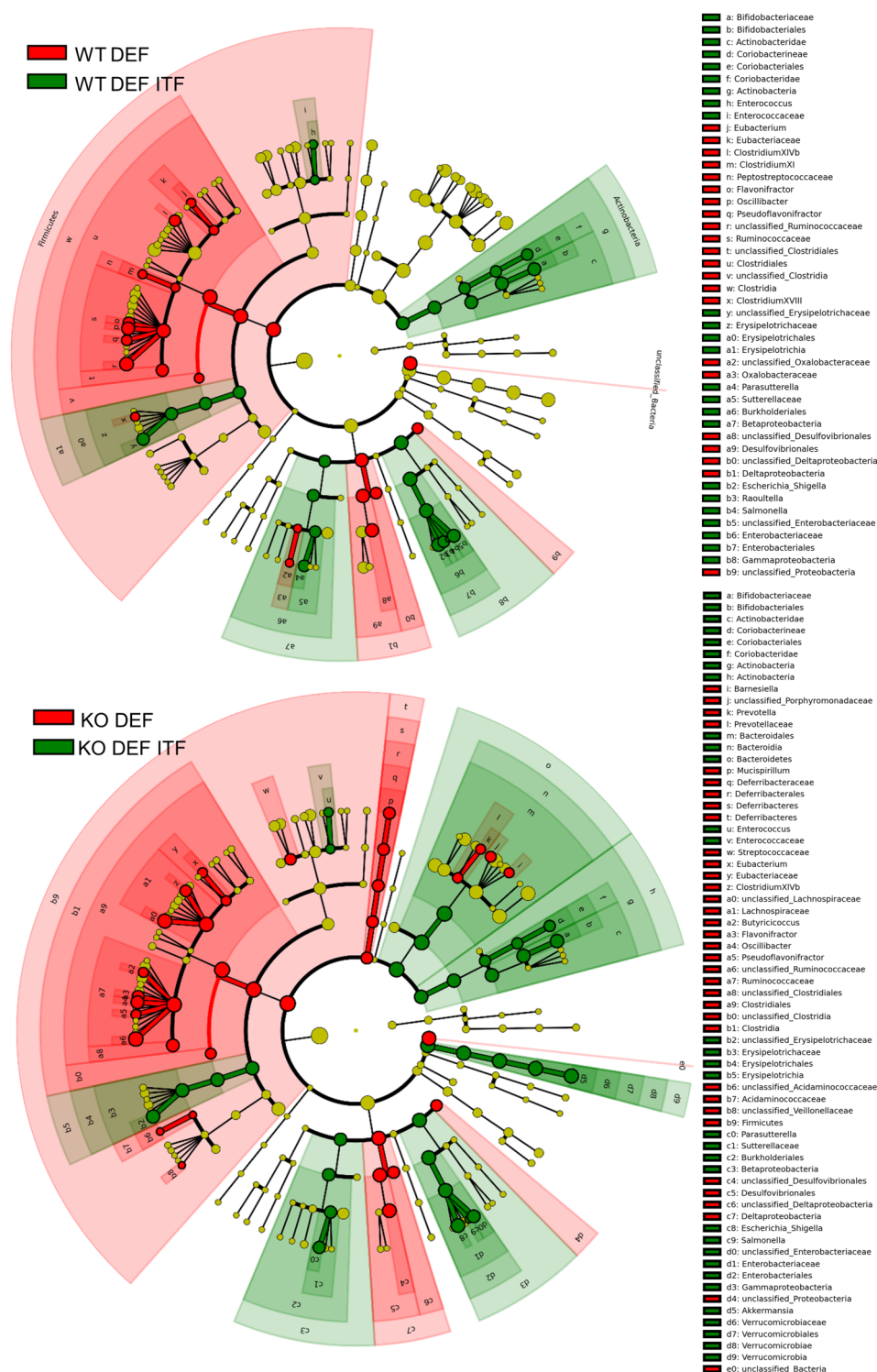


Figure 4 Inulin-type fructans (ITF) treatment profoundly modifies the composition of the caecal microbiota. (A) Shannon and Simpson Indexes. (B) Simpson Evenness and Heip Indexes. (C) Chao1 and Observed Species Indexes. (D) Principal coordinates analysis (PCoA) of Morisita-Horn Index and (E) of weighted UniFrac Index at the operational taxonomic unit (OTU) level (Adonis method, 1000 permutations, $p < 0.001$ for both PCoAs). (F) Pie charts presenting the relative mean abundance of phyla. (G) Relative abundance of the most increased bacterial taxa by ITF treatment. (H) Relative abundance of the most decreased bacterial taxa by ITF treatment. Data ($N=15-18$) are expressed as mean \pm SEM and analysed by one-way analysis of variance followed by Tukey's post-tests: * versus WT DEF, \$ versus WT DEF ITF, # versus KO DEF.

in KO DEF mice while the ITF treatment restored its abundance to a similar level as observed in WT mice (figure 4G). Concomitantly, ITFs also led to a decreased relative abundance of Desulfovibrionales and Clostridiales orders and of the Ruminococcaceae and Lachnospiraceae families (only in the KO genotype for the last family) (figure 4H). Discriminant analyses

using LefSe confirmed these results (figure 5). Enrichment in Actinobacteria (Bifidobacteriales and Coriobacteriales orders), Enterobacteriaceae and Erysipelotrichaceae characterised ITF-treated mice whereas enrichment in Deltaproteobacteria, Ruminococcaceae and Clostridiales was observed in untreated mice (figure 5 and see online supplementary figure S2). It

Figure 5 LEfSe cladograms reveal enrichment in several bacterial taxa upon prebiotic supplementation. Discriminant analyses using LEfSe. Bacterial taxa enriched in inulin-type fructans (ITF)-treated mice appear in green and bacterial taxa enriched in untreated mice appear in red.



appears from visual comparison of cladograms that ITFs have similar but not identical effects in both genotypes, with a few changes occurring only in KO DEF groups (such as enrichment in Bacteroidetes and *Akkermansia* upon ITFs). Among the 93 OTUs significantly modified by the treatments at the q-level, OTU 19, identified as *Escherichia coli*, and OTU 6, identified as *Shigella boydii*, were increased by at least 600-fold, in ITF-treated groups (see online supplementary table S1). Moreover, OTU 1, identified as *Akkermansia muciniphila*, was increased by fourfold in KO DEF ITF versus KO DEF mice, reaching 16% of the gut microbiota in KO DEF ITF mice. We also observed that six OTUs,

all belonging to the Lachnospiraceae family, were drastically decreased by ITFs in both genotypes (between 127-fold and 2198-fold decrease, mostly observed in KO DEF ITF). OTU 141, identified as unclassified Ruminococcaceae, also decreased by 217-fold in KO DEF ITF as compared with KO DEF mice (see online supplementary table S1).

ITF treatment quantitatively and qualitatively modifies plasma and caecal BA profiles

We measured the expression of genes involved in the biosynthesis and enterohepatic cycle of BAs focusing on KO genotype,

which develop the endothelial dysfunction. ITF supplementation significantly upregulated hepatic mRNA levels of *Cyp7a1*, the rate-limiting enzyme of the classical BA synthesis pathway (figure 6A). Although *Cyp27a1*, which is mostly involved in the alternative pathway, was not affected by ITF treatment, the expression of *Cyp7b1* was decreased by ITF treatment. *Cyp8b1* was not modified by the ITF supplementation (figure 6A). ITF treatment significantly enhanced markers of BAs reuptake in the ileum (*Slc10a2*, *Fabp6*, *Slc51a/b*) (figure 6B). ITF treatment also increased the BA concentration, which was mainly due to the rise in free BAs, rather than the tauro-conjugated BAs (figure 6C–F). More precisely, the primary BAs cholic acid (CA) and chenodeoxycholic acid (CDCA) increased strongly in the portal and systemic blood as well as in the caecal content. Muricholic acid (MCA) and ursodeoxycholic acid (UDCA) were also strongly increased in blood and in caecal content. In contrast, the concentrations of the secondary BA deoxycholic acid (DCA) and its tauro-conjugated form were strongly reduced following ITF supplementation. Another secondary BA, lithocholic acid (LCA), was also significantly decreased in the caecal content by the ITF treatment (figure 6H). Caecal DCA and LCA positively correlated with abundance in unclassified Ruminococcaceae and with abundance in Lachnospiraceae and unclassified Lachnospiraceae (figure 7 and see online supplementary figure S3 and table S2). A PICRUSt analysis predicted no significant difference in primary and secondary BA biosynthesis pathways (see online supplementary table S3). These results must be taken into account with caution because of the moderate accuracy of the prediction, evidenced by a mean NSTI value of 0.10 ± 0.006 .²⁷ Since *Cyp7a1* also regulates cholesterol metabolism and its enteric elimination, we determined blood lipid profiles in KO DEF and KO DEF ITF mice. ITF treatment did not modify the plasma lipids profile (see online supplementary table S4).

ITF treatment increases glucagon-like peptide 1 production

ITF treatment in KO DEF ITF mice provoked a threefold increase in active portal glucagon-like peptide 1 (GLP-1) concentrations, as compared with KO DEF mice (figure 8A). Increased expression of *Gcg* and of an enzyme involved in GLP-1 maturation (namely prohormone convertase 1/3, *PC1/3*) were observed in KO DEF ITF mice (figure 8B). Differentiation factors *NeuroD1* and neurogenin 3 (*Ng3*) were not modified by ITF treatment, suggesting they are not involved in higher differentiation of enteroendocrine cells producing GLP-1. However, a large number of GLP-1-positive cells was observed in the proximal colon, thereby suggesting that overall pool of L cells is increased whereas the differentiation is not affected (figure 8C,D).²⁸ Accordingly, correlation analysis revealed that *Gcg* mRNA positively correlates with the abundance of Bifidobacteriaceae and Verrucomicrobiaceae families, both enhanced by ITFs, and negatively correlates with the abundance of Ruminococcaceae and Lachnospiraceae families (figure 8E).

DISCUSSION

Metabolic diseases such as non-alcoholic fatty liver disease are associated with macro- and microcirculation and microcirculation damage, initiating an impairment of endothelium-dependent relaxation.^{19 29} Here, we demonstrate that supplementation in ITF for 15 days corrects the endothelial dysfunction – an early key biomarker of CVDs – present in n-3 PUFA-depleted *Apoe*^{−/−} mice.

Blood vessels are assumed to respond to varying conditions and functional demands through continuous adaptive structural changes. Accordingly following ITF treatment, we observed an

increase in mesenteric diameter and wall thickness associated with increasing contractile reactivity, all needed to ensure stable vascular adaptation. Interestingly, the favourable outward remodelling, observed locally, was also characterised by improved NO-dependent endothelium relaxation. In most cases, endothelial dysfunction is related to a reduced NO availability in mice.³⁰ Inhibiting the NOS/NO pathway with L-NAME totally masked the vasodilation in mice, abolishing the positive effect of ITFs. The increased ratio of p-eNOS^{ser1177} to total eNOS suggests that ITFs activate the NOS/NO pathway in *Apoe*^{−/−} mice.

Of more relevance for human CVD, effects of ITFs were not restricted to the enteric vascular tree, such effects were also observed at a distance from the mesenteric bed as indicated by the recovery of the circulating level of Hb-NO in peripheral blood and the improved relaxation in carotid arteries. Whether the molecular mechanisms underlying the improved NO-dependent relaxation in the carotid artery fully reflect those involved in the mesenteric tree remains elusive at this stage.

Weight loss can improve the impairment of endothelium-dependent relaxation;³¹ however, this hypothesis can be ruled out in our study as no change in body weight was observed in ITF-treated versus untreated mice (see online supplementary table S5).

The Erysipelotrichaceae family, belonging to the Firmicutes phylum, was expanded by ITFs. It has been previously reported that dietary intervention such as prebiotics or berberine in high-fat-fed mice concomitantly led to an expanded abundance of *Allobaculum* sp – an important member of the Erysipelotrichaceae family – and to an improvement in metabolic parameters, suggesting a potential beneficial contribution of *Allobaculum* sp to host phenotype.^{32 33} In agreement with these observations, ITFs increased OTU 4, closely related to *Allobaculum* sp (90.4%), by tenfold in ITF-treated *Apoe*^{−/−} mice. Furthermore, abundance in Erysipelotrichaceae was strongly and positively correlated with portal CDCA, UDCA and MCAs but not to their conjugates.

Abundance of *Akkermansia*, a bacterium capable of reducing fat mass development, insulin resistance and dyslipidaemia in obese mice,^{11 12} was quadrupled by ITFs in *Apoe*^{−/−} mice, reaching the same level as that observed in WT mice. In addition, it has been reported that *Akkermansia* positively correlates with higher levels of circulating primary BAs;³⁴ it is in accordance with the positive correlation observed between circulating CA and this bacterium. Based on the results of multiple correlation analyses, we propose that the marked decreases in the Lachnospiraceae and Ruminococcaceae families caused by ITFs contribute to the drop in DCA and LCA concentration, since they are among the dominant families able to produce secondary BAs through 7 α -dehydroxylation. These observations are consistent with previous studies showing, in humans and mice with liver diseases, an association between abundance of Ruminococcaceae and Lachnospiraceae families and secondary BA concentrations.^{35 36} The Desulfovibrionales order, known to be increased by high-fat diet and associated with inflammation and/or altered gut barrier in mouse models,^{33 37 38} was also decreased by at least twofold in ITF-supplemented mice and strongly correlated with DCA concentration in *Apoe*^{−/−} mice. We can therefore propose that changing the microbial composition using ITFs impacts largely the production of secondary BAs and could contribute to the improvement of the host's health.

Changes in BA profiles by ITF treatment also result from the modulation of BA metabolism, including hepatic synthesis (in

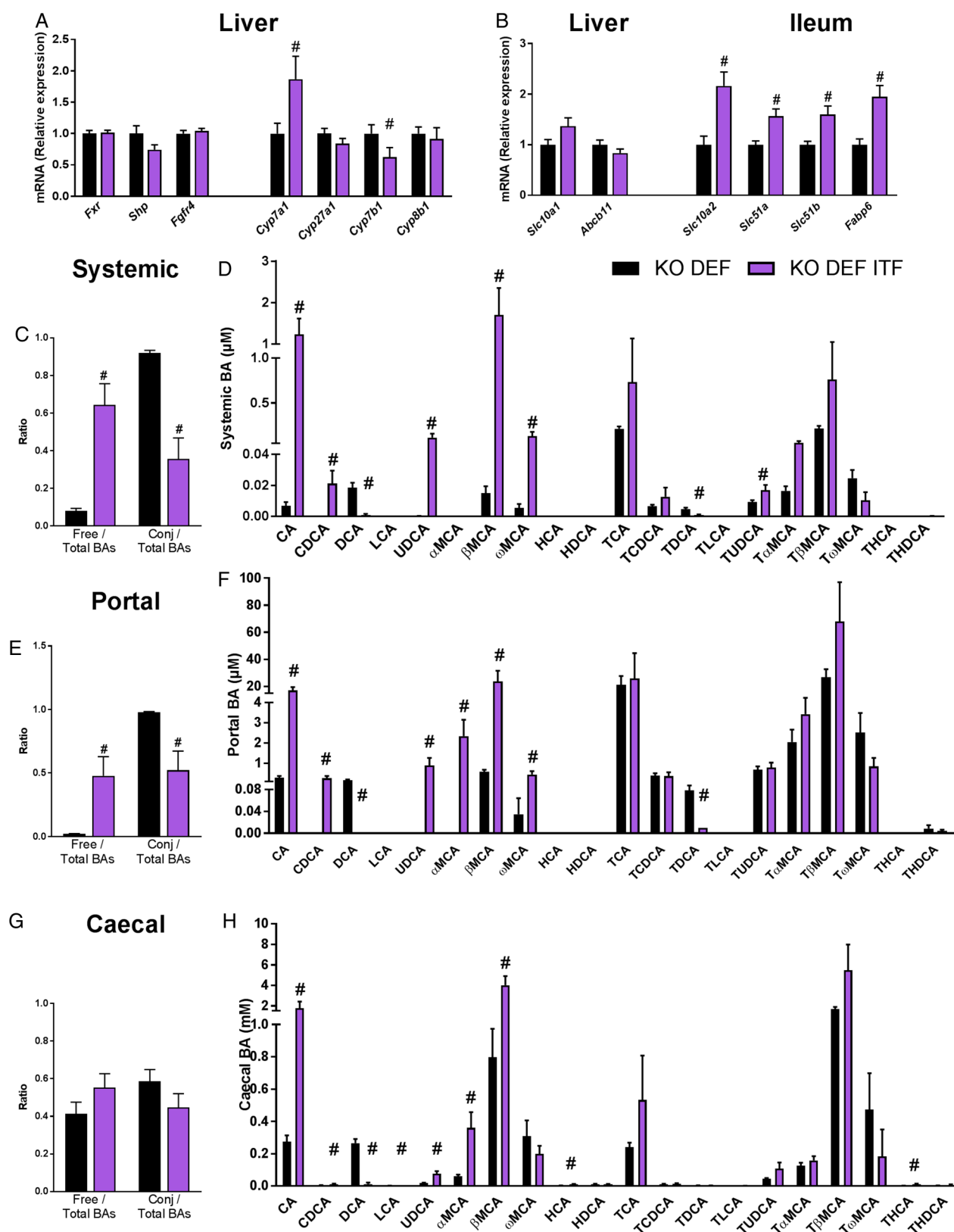
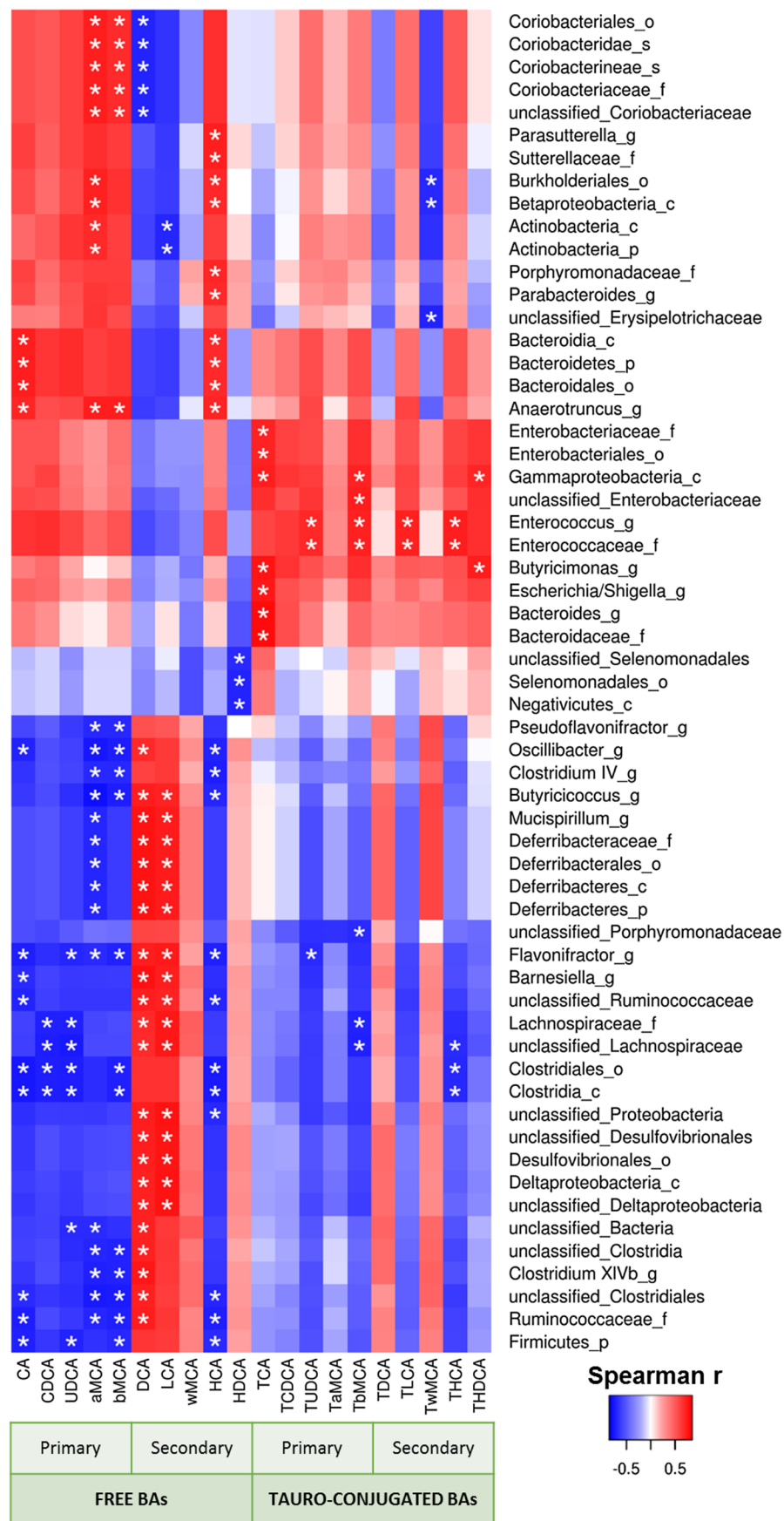


Figure 6 Bile acid (BA) metabolism affected by inulin-type fructans (ITF) supplementation in KO genotype. (A) Genes involved in BA biosynthesis and its regulation (N=11–12). (B) Genes involved in the enterohepatic cycle (N=8–12). (C) Ratio of free and conjugated to total BAs in systemic blood (N=6). (D) Systemic BA profile (N=6). (E) Ratio of free and conjugated to total BAs in portal blood (N=5–6). (F) Portal BA profile (N=5–6). (G) Ratio of free and conjugated to total BAs in caecal content (N=6). (H) Caecal BA profile (N=6). Data are expressed as mean±SEM and analysed by unpaired *t*-test; # versus KO DEF.

Figure 7 Heatmap representation of the Spearman's r correlation coefficient between caecal bile acid profile and bacterial taxa. Only the bacteria, for which at least one significant correlation to bile acid levels was found, are displayed (c, class; o, order; f, family; g, genus; s, species).
*Adjusted p value <0.05.



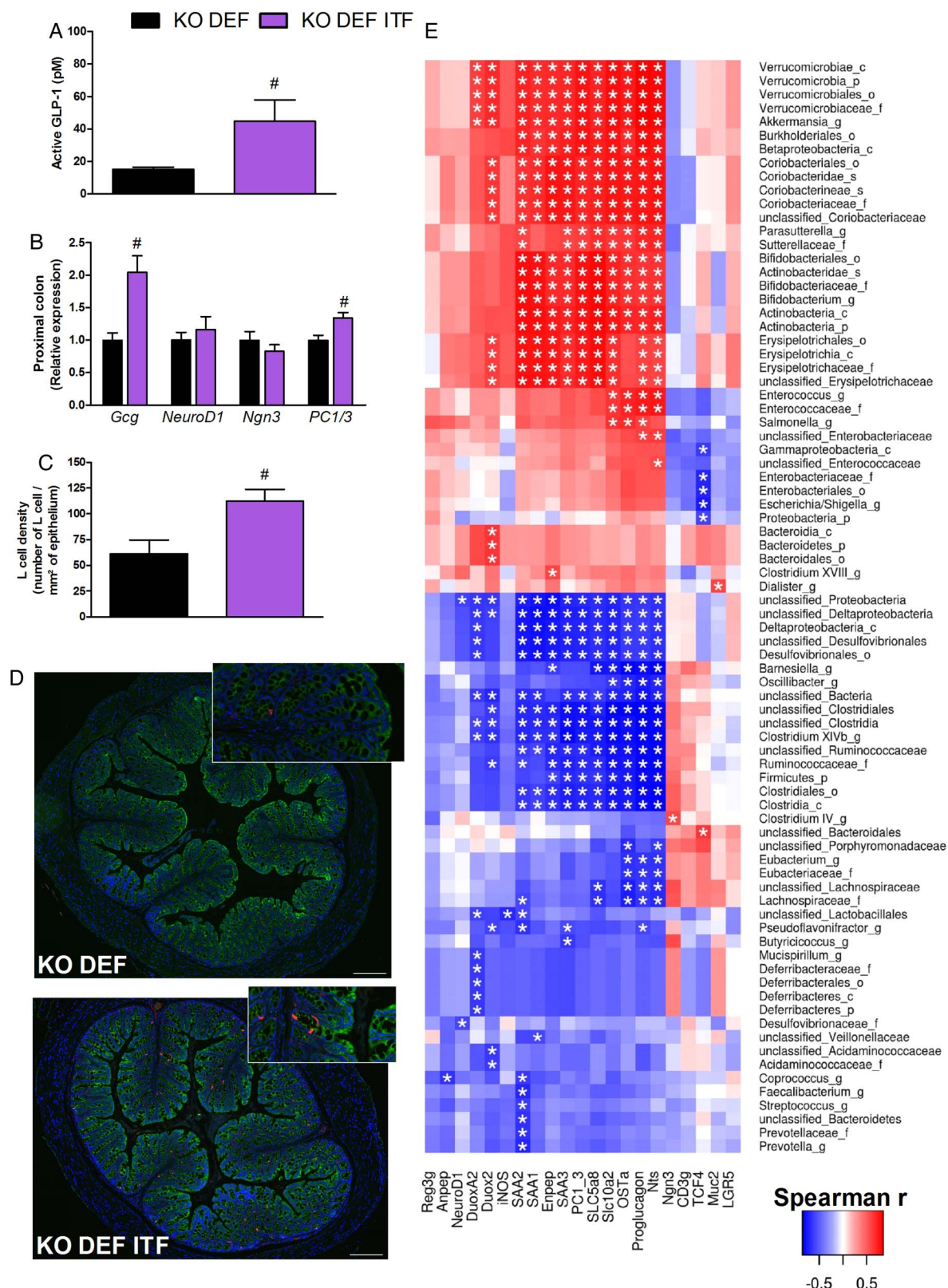


Figure 8 Prebiotic treatment increases glucagon-like peptide 1 (GLP-1) production. (A) Active GLP-1 concentration (N=9–10). (B) Proglucagon (*Gcg*), *NeuroD1*, neurogenin 3 (*Ngn3*) and prohormone convertase 1/3 (*PC1/3*) expression in proximal colon (N=7–8). (C) L cell density in proximal colon (N=6–8). (D) Representative immunofluorescence staining for L cell density. CK8+18 (green), GLP-1 (red) and DNA (blue) in proximal colon (scale bar=200 μm). Data are expressed as mean±SEM and analysed by unpaired *t*-test: # versus KO n-3 PUFA-depleted (DEF). (E) Heatmap representation of the Spearman's *r* correlation coefficient between caecal expression of gene highlighted by the microarray analysis and confirmed by qPCR, and bacterial taxa. Only the bacteria for which at least one significant correlation to genes expression was found, are displayed (c, class; o, order; f, family; g, genus; s, species). *Adjusted p value < 0.05.

favour of *Cyp7a1*) and intestinal reuptake. In the liver, BA-activated Farnesoid X receptor (*FXR*) induces the expression of small heterodimer partner (*Shp*) which can inhibit *Cyp7a1* expression; both are negatively correlated in our study (Spearman's $r = -0.62$; $p = 0.0014$). Although *FXR* mRNA expression was not affected by ITFs, α and β MCAs (free or tauro-conjugated) induced by ITFs, have *FXR* antagonistic properties^{39 40} and may contribute to the *Cyp7a1* upregulation. In addition, ITFs enhance BA reabsorption, which is negatively associated with changes in Ruminococcaceae and Lachnospiraceae families and positively associated with the Bifidobacteriaceae and Erysipelotrichaceae families and the *Akkermansia* genus.

Enterobacteriaceae were largely expanded by the ITF supplementation and were dominated by *E coli/Shigella* (identified as OTUs 19 and 6, respectively) in our study. Interestingly, bacteria like *E coli*, can produce NO either enzymatically from L-arginine via bacterial NOS or non-enzymatically through nitrite reduction.^{41 42} Another bacterial family increased by ITFs that may contribute to NO generation is the Bifidobacteriaceae family. Indeed, by decreasing the pH, bifidobacteria may generate more NO than any other species through the acidic non-enzymatic reduction of nitrite.⁴³

The promotion of GLP-1 release by ITFs appears to be another potential link between events occurring in the bacterial ecosystem and improvement of endothelial function, since *Bifidobacterium* as well as *Akkermansia* are positively correlated with mRNA expression of *Gcg* and *Nts*, being coexpressed and co-released with GLP-1.⁴⁴ Moreover, GLP-1 infusion or GLP-1 receptor agonists can correct endothelial dysfunction, in humans and rodents, by reducing oxidative stress or by activating the NOS/NO pathway via eNOS phosphorylation.^{45–47}

BAs produced through metabolic cooperation between hosts and microbes, may improve endothelial dysfunction through the TGR5 receptor pathway^{48 49} as has been extensively reported in Fiorucci *et al.*⁴⁹ We confirmed that free BAs such as CA, CDCA and UDCA directly stimulate the NOS/NO pathway by enhancing serine phosphorylation of eNOS in vitro (data not shown). In addition, TGR5 is highly expressed in enteroendocrine L cells in the small intestine and stimulates GLP-1 secretion, thus indirectly improving the endothelial function.^{49 50} Plasmatic LDLc and HDLc levels were similar in all groups of mice. Although lipid profiles were measured in mice that were not rigorously fasted, and therefore might be not completely accurate, it is very unlikely that different lipoprotein plasma levels contributed to the beneficial effects of ITFs.

The improvement of enteric vascular dysfunction by ITFs could relate to events occurring at microbial level (e.g. increase in NO-producing bacteria) and/or at host level (e.g. changes in BA composition, increase in L cells density and GLP-1 production, both acting on the NOS/NO pathway).

Our study is the first to point out the effects of ITFs on host cardiometabolic health, including endothelial and endocrine functions, and can be considered as a rationale to evaluate such an effect in a human intervention study. For sure, the dose at which ITF would be tested is below the one given to animals (0.25 g/day). In human intervention studies, doses ranging from 12g/day to 16 g/day are often given when testing for metabolic effects of ITF.^{51–54} In addition, there are certainly differences between humans and mice concerning the gut microbiota composition, but it is rather interesting to point out that similar bacterial changes occur in both humans and mice upon prebiotic intervention (e.g. in favour of the *Bifidobacterium* genus).^{55 56} While effects on gut function (e.g. increase in GLP-1 production

by prebiotics) have been largely described in rodent models, several papers also reported the influence of prebiotics in humans.^{51–54}

In conclusion, our findings pave the way for innovative therapeutic approaches in prevention of human vascular dysfunction, for which no treatment has been successfully proposed so far.

Author affiliations

¹Metabolism and Nutrition Research Group, Louvain Drug Research Institute, Université catholique de Louvain, Brussels, Belgium

²European Genomic Institute for Diabetes (EGID), Univ Lille, Lille, France

³INSERM UMR 1011, Lille, France

⁴Institut Pasteur de Lille, Lille, France

⁵CHU de Lille, Lille, France

⁶Centre Universitaire de Mesures et d'Analyses, Univ. Lille, Lille, France

⁷EA 7365 GRITA, Lille, France

⁸Pole of Pharmacology and Therapeutics, Institut de Recherche Expérimentale et Clinique, Université catholique de Louvain, Brussels, Belgium

⁹Wallon Excellence in Life sciences and Biotechnology (WELBIO), Belgium

¹⁰Pole of Experimental Medicine, de Duve Institute, Université catholique de Louvain, Brussels, Belgium

¹¹IREC Imaging Platform, Université catholique de Louvain, Brussels, Belgium

Twitter Follow Patrice Cani @MicObesity

Acknowledgements The authors thank B Es Saadi and R Selleslagh for technical assistance and V Joris for in vitro analyses.

Contributors Conceptualisation: EC, CD and NMD; Methodology: EC, CD and NMD; Investigation: EC, LBB, AT, SL, AMN, IL, CB, PDC and BS; Formal analysis: J-FG, HP, AE and J-BD; Writing-original draft: EC, CD and NMD; Writing review and editing: all the authors; Supervision: CD and NMD.

Funding This work is supported by FNRS (Fond National de la Recherche Scientifique, Belgium; CDR J.0122.15). LBB was a postdoctoral researcher from the FRS-FNRS and is the recipient of subsidies from the FSR (Fonds Spéciaux de la Recherche, UCL). HP is a research fellow at the FRS-FNRS. NMD is a recipient of grants from FRS-FNRS, from Wallonia supported by the competitive cluster Wagralim (ADIPOSTOP project, convention 7366; FOOD4GUT project, convention 1318148) and from the European Union's Seventh Framework Program (grant agreement no 613979). PDC is a research associate at the FRS-FNRS and the recipient of grants from FNRS (convention J.0084.15, convention 3.4579.11), PDC (Projet de Recherche, convention: T.0138.14), WELBIO-CR-2012S-02R, the Funds Baillet Latour (Grant for Medical Research 2015). PDC is a recipient of an ERC Starting Grant 2013 (starting grant 336452-ENIGMO). CD is a senior research associate at FRS-FNRS. BS is a recipient of the Institut Universitaire de France. This work was partly supported by grants from the European Genomic Institute for Diabetes (ANR-10-LABX-46) and the ERC Grant (Immunobile, contract 694717).

Competing interests None declared.

Ethics approval The experiments were approved by and performed in accordance with the guidelines of the local ethics committee. Housing conditions were as specified by the Belgian Law of 29 May 2013, regarding the protection of laboratory animals (agreement no LA1230314).

Provenance and peer review Not commissioned; externally peer reviewed.

Open Access This is an Open Access article distributed in accordance with the Creative Commons Attribution Non Commercial (CC BY-NC 4.0) license, which permits others to distribute, remix, adapt, build upon this work non-commercially, and license their derivative works on different terms, provided the original work is properly cited and the use is non-commercial. See: <http://creativecommons.org/licenses/by-nc/4.0/>

REFERENCES

- 1 Mozaffarian D, Benjamin EJ, Go AS, *et al.* Heart disease and stroke statistics—2015 update: a report from the American Heart Association. *Circulation* 2015;131:e29–322.
- 2 Cordain L, Eaton SB, Sebastian A, *et al.* Origins and evolution of the Western diet: health implications for the 21st century. *Am J Clin Nutr* 2005;81:341–54.
- 3 WHO. *Cardiovascular diseases (CVDs). Fact sheet.* 2016 edn. Geneva, Switzerland, 2016.
- 4 Brunner H, Cockcroft JR, Deanfield J, *et al.* Endothelial function and dysfunction. Part II: association with cardiovascular risk factors and diseases. A statement by the Working Group on Endothelins and Endothelial Factors of the European Society of Hypertension. *J Hypertens* 2005;23:233–46.

- 5 Juonala M, Viikari JS, Laitinen T, *et al.* Interrelations between brachial endothelial function and carotid intima-media thickness in young adults: the cardiovascular risk in young Finns study. *Circulation* 2004;110:2918–23.
- 6 Catry E, Neyrinck AM, Lobysheva I, *et al.* Nutritional depletion in n-3 PUFA in apoE knock-out mice: a new model of endothelial dysfunction associated with fatty liver disease. *Mol Nutr Food Res* 2016;60:2198–207.
- 7 Delzenne NM, Cani PD, Everard A, *et al.* Gut microorganisms as promising targets for the management of type 2 diabetes. *Diabetologia* 2015;58:2206–17.
- 8 Qin J, Li R, Raes J, *et al.* A human gut microbial gene catalogue established by metagenomic sequencing. *Nature* 2010;464:59–65.
- 9 Stepankova R, Tonar Z, Bartova J, *et al.* Absence of microbiota (germ-free conditions) accelerates the atherosclerosis in ApoE-deficient mice fed standard low cholesterol diet. *J Atheroscler Thromb* 2010;17:796–804.
- 10 Rault-Nania MH, Gueux E, Demougeot C, *et al.* Inulin attenuates atherosclerosis in apolipoprotein E-deficient mice. *Br J Nutr* 2006;96:840–4.
- 11 Everard A, Belzer C, Geurts L, *et al.* Cross-talk between Akkermansia muciniphila and intestinal epithelium controls diet-induced obesity. *Proc Natl Acad Sci USA* 2013;110:9066–71.
- 12 Plovier H, Everard A, Druart C, *et al.* A purified membrane protein from Akkermansia muciniphila or the pasteurized bacterium improves metabolism in obese and diabetic mice. *Nat Med* 2017;23:107–13.
- 13 Li J, Lin S, Vanhoutte PM, *et al.* Akkermansia muciniphila protects against atherosclerosis by preventing metabolic endotoxemia-induced inflammation in ApoE $-/-$ mice. *Circulation* 2016;133:2434–46.
- 14 Delzenne NM, Neyrinck AM, Cani PD. Gut microbiota and metabolic disorders: How prebiotic can work? *Br J Nutr* 2013;109 2):S81–5.
- 15 Delzenne NM, Neyrinck AM, Cani PD. Modulation of the gut microbiota by nutrients with prebiotic properties: consequences for host health in the context of obesity and metabolic syndrome. *Microb Cell Fact* 2011;10(Suppl 1):S10.
- 16 Bindels LB, Delzenne NM, Cani PD, *et al.* Towards a more comprehensive concept for prebiotics. *Nat Rev Gastroenterol Hepatol* 2015;12:303–10.
- 17 Pachikian BD, Essaghir A, Demoulin JB, *et al.* Prebiotic approach alleviates hepatic steatosis: implication of fatty acid oxidative and cholesterol synthesis pathways. *Mol Nutr Food Res* 2013;57:347–59.
- 18 Kim JA, Montagnani M, Koh KK, *et al.* Reciprocal relationships between insulin resistance and endothelial dysfunction: molecular and pathophysiological mechanisms. *Circulation* 2006;113:1888–904.
- 19 Francque SM, van der Graaff D, Kwanten WJ. Non-alcoholic fatty liver disease and cardiovascular risk: pathophysiological mechanisms and implications. *J Hepatol* 2016;65:425–43.
- 20 Essaghir A, Dif N, Marbehan CY, *et al.* The transcription of FOXO genes is stimulated by FOXO3 and repressed by growth factors. *J Biol Chem* 2009;284:10334–42.
- 21 Bindels LB, Neyrinck AM, Claus SP, *et al.* Synbiotic approach restores intestinal homeostasis and prolongs survival in leukaemic mice with cachexia. *ISME J* 2016;10:1456–70.
- 22 Eren AM, Vineis JH, Morrison HG, *et al.* A filtering method to generate high quality short reads using illumina paired-end technology. *PLoS ONE* 2013;8:e66643.
- 23 Schloss PD, Westcott SL, Ryabin T, *et al.* Introducing mothur: open-source, platform-independent, community-supported software for describing and comparing microbial communities. *Appl Environ Microbiol* 2009;75:7537–41.
- 24 Edgar RC. UPARSE: highly accurate OTU sequences from microbial amplicon reads. *Nat Methods* 2013;10:996–8.
- 25 Cole JR, Wang Q, Fish JA, *et al.* Ribosomal Database Project: data and tools for high throughput rRNA analysis. *Nucleic Acids Res* 2014;42(Database issue):D633–42.
- 26 Pelat M, Dessy C, Massion P, *et al.* Rosuvastatin decreases caveolin-1 and improves nitric oxide-dependent heart rate and blood pressure variability in apolipoprotein E $-/-$ mice in vivo. *Circulation* 2003;107:2480–6.
- 27 Langille MG, Zaneveld J, Caporaso JG, *et al.* Predictive functional profiling of microbial communities using 16S rRNA marker gene sequences. *Nat Biotechnol* 2013;31:814–21.
- 28 Everard A, Lazarevic V, Derrien M, *et al.* Responses of gut microbiota and glucose and lipid metabolism to prebiotics in genetic obese and diet-induced leptin-resistant mice. *Diabetes* 2011;60:2775–86.
- 29 Tilg H, Moschen AR, Roden M. NAFLD and diabetes mellitus. *Nat Rev Gastroenterol Hepatol* 2017;14:32–42.
- 30 d'Uscio LV, Baker TA, Mantilla CB, *et al.* Mechanism of endothelial dysfunction in apolipoprotein E-deficient mice. *Arterioscler Thromb Vasc Biol* 2001;21:1017–22.
- 31 Bigornia SJ, Mott MM, Hess DT, *et al.* Long-term successful weight loss improves vascular endothelial function in severely obese individuals. *Obesity (Silver Spring)* 2010;18:754–9.
- 32 Zhang X, Zhao Y, Zhang M, *et al.* Structural changes of gut microbiota during berberine-mediated prevention of obesity and insulin resistance in high-fat diet-fed rats. *PLoS one* 2012;7:e42529.
- 33 Everard A, Lazarevic V, Gaia N, *et al.* Microbiome of prebiotic-treated mice reveals novel targets involved in host response during obesity. *ISME J* 2014;8:2116–30.
- 34 Pierre JF, Martinez KB, Ye H, *et al.* Activation of bile acid signaling improves metabolic phenotypes in high-fat diet-induced obese mice. *Am J Physiol Gastrointest Liver Physiol* 2016;311:G286–304.
- 35 Liu HX, Rocha CS, Dandekar S, *et al.* Functional analysis of the relationship between intestinal microbiota and the expression of hepatic genes and pathways during the course of liver regeneration. *J Hepatol* 2016;64:641–50.
- 36 Kakiyama G, Pandak WM, Gillevet PM, *et al.* Modulation of the fecal bile acid profile by gut microbiota in cirrhosis. *J Hepatol* 2013;58:949–55.
- 37 Lam YY, Ha CW, Campbell CR, *et al.* Increased gut permeability and microbiota change associate with mesenteric fat inflammation and metabolic dysfunction in diet-induced obese mice. *PLoS ONE* 2012;7:e34233.
- 38 Loubinoux J, Bronowicki JP, Pereira IA, *et al.* Sulfate-reducing bacteria in human feces and their association with inflammatory bowel diseases. *FEMS Microbiol Ecol* 2002;40:107–12.
- 39 Sayin SI, Wahlström A, Felin J, *et al.* Gut microbiota regulates bile acid metabolism by reducing the levels of tauro-beta-muricholic acid, a naturally occurring FXR antagonist. *Cell Metab* 2013;17:225–35.
- 40 Wahlström A, Sayin SI, Marschall HU, *et al.* Intestinal crosstalk between Bile acids and Microbiota and its impact on host metabolism. *Cell Metab* 2016;24: 41–50.
- 41 Sudhamsu J, Crane BR. Bacterial nitric oxide synthases: what are they good for? *Trends Microbiol* 2009;17:212–8.
- 42 Vermeiren J, Van de Wiele T, Verstraete W, *et al.* Nitric oxide production by the human intestinal microbiota by dissimilatory nitrate reduction to ammonium. *J Biomed Biotechnol* 2009;2009:284718.
- 43 Sobko T, Reinders CI, Jansson E, *et al.* Gastrointestinal bacteria generate nitric oxide from nitrate and nitrite. *Nitric Oxide* 2005;13:272–8.
- 44 Grunddal KV, Ratner CF, Svendsen B, *et al.* Neurotensin is coexpressed, coreleased, and acts together with GLP-1 and PYY in enteroendocrine control of metabolism. *Endocrinology* 2016;157:176–94.
- 45 Lovshin J, Cherney D. GLP-1R agonists and endothelial dysfunction: more than just glucose lowering? *Diabetes* 2015;64:2319–21.
- 46 Subaran SC, Sauder MA, Chai W, *et al.* GLP-1 at physiological concentrations recruits skeletal and cardiac muscle microvasculature in healthy humans. *Clin Sci (Lond)* 2014;127:163–70.
- 47 Cantini G, Mannucci E, Luconi M. Perspectives in GLP-1 research: new targets, new receptors. *Trends Endocrinol Metab* 2016;27:427–38.
- 48 Kida T, Tsubosaka Y, Hori M, *et al.* Bile acid receptor TGR5 agonism induces NO production and reduces monocyte adhesion in vascular endothelial cells. *Arterioscler Thromb Vasc Biol* 2013;33:1663–9.
- 49 Fiorucci S, Zampella A, Cirino G, *et al.* Decoding the vasoregulatory activities of bile acid activated receptors in systemic and portal circulation. Role for gaseous mediators. *Am J Physiol Heart Circ Physiol* 2017;312:H21–32.
- 50 Trabelsi MS, Daoudi M, Prawitt J, *et al.* Farnesoid X receptor inhibits glucagon-like peptide-1 production by enteroendocrine L cells. *Nat Commun* 2015;6:7629.
- 51 Cani PD, Lecourt E, Dewulf EM, *et al.* Gut microbiota fermentation of prebiotics increases satiety and incretin gut peptide production with consequences for appetite sensation and glucose response after a meal. *Am J Clin Nutr* 2009;90:1236–43.
- 52 Parnell JA, Reimer RA. Weight loss during oligofructose supplementation is associated with decreased ghrelin and increased peptide YY in overweight and obese adults. *Am J Clin Nutr* 2009;89:1751–9.
- 53 Rahat-Rozenbloom S, Fernandes J, Cheng J, *et al.* Acute increases in serum colonic short-chain fatty acids elicited by inulin do not increase GLP-1 or PYY responses but may reduce ghrelin in lean and overweight humans. *Eur J Clin Nutr* 2016.
- 54 Tarini J, Wolever TM. The fermentable fibre inulin increases postprandial serum short-chain fatty acids and reduces free-fatty acids and ghrelin in healthy subjects. *Appl Physiol Nutr Metab* 2010;35:9–16.
- 55 Dewulf EM, Cani PD, Claus SP, *et al.* Insight into the prebiotic concept: lessons from an exploratory, double blind intervention study with inulin-type fructans in obese women. *Gut* 2013;62:1112–21.
- 56 Vulevic J, Juric A, Tzortzis G, *et al.* A mixture of trans-galactooligosaccharides reduces markers of metabolic syndrome and modulates the fecal microbiota and immune function of overweight adults. *J Nutr* 2013;143:324–31.